THREE ISOPARAMETRIC SOLID ELEMENTS FOR NASTRAN

By   Stephen E. Johnson and Eric I. Field

Universal Analytics, Inc.
Los Angeles, California

SUMMARY

Linear, quadratic, and cubic isoparametric hexahedral solid elements have been added to the element library of NASTRAN. These elements are available for static, dynamic, buckling, and heat-transfer analyses. Because the isoparametric element matrices are generated by direct numerical integration over the volume of the element, variations in material properties, temperatures, and stresses within the elements are represented in the computations. In order to compare the accuracy of the new elements, three similar models of a slender cantilever were developed, one for each element. All elements performed well. As expected, however, the linear element model yielded excellent results only when shear behavior predominated. In contrast, the results obtained from the quadratic and cubic element models were excellent in both shear and bending.

INTRODUCTION

New aerospace vehicle concepts, such as the Space Shuttle, have added impetus for the continued updating of NASTRAN with the best state-of-the-art finite element technology. In response to this need, the three-dimensional family of linear, quadratic, and cubic isoparametric hexahedral solid elements were developed for and installed in NASTRAN. These three new elements significantly improve NASTRAN's capability to solve any three-dimensional solid problem requiring static, dynamic, buckling, and/or heat-transfer analysis.

THEORETICAL BACKGROUND

Hexahedron solid isoparametric elements may be used to analyze any three-dimensional continuum composed of isotropic or anisotropic materials. Examples include thick inserts in rocket engine nozzles, thermal protection system insulations, soil structure interaction problems, and geometrically complex thick-walled mechanical components such as pumps, valves, etc. These solid elements have only three degrees of freedom at each grid point (the three displacement components), and they may be combined with all other nonaxisymmetric NASTRAN elements.

The isoparametric solid elements were first presented by Irons, Ergatoudis and Zienkiewicz [Refs. 1 to 4]. Isoparametric solid elements employing either eight, twenty or thirty-two grid points have been found to be suitable to solve most problems (Figure 1). These elements correspond to assuming a linear, quadratic, and cubic variation of displacement, respectively. Clough [Ref. 5] conducted an evaluation of three-dimensional solid elements and showed that the isoparametric elements were superior to other solid elements. He further

pointed out that the choice of which isoparametric element is best to use depends on the type of problem being solved. For problems involving shear and bending type deformations, the higher order elements are preferred over the linear elements which should be used for problems in which shear stresses predominate. It is for this reason that all three isoparametric elements have been incorporated into NASTRAN.

The governing equations for isoparametric elements are based on minimum energy principles. The derivation of these equations assumes a displacement function over the element which depends on grid point displacements only. The governing equations are obtained by minimizing the Potential Energy which is evaluated in terms of these displacement functions.

Displacement Functions

The name isoparametric is derived from the fact that the interpolating or shape functions used to represent the deformation of the element are also used to represent the geometry of the element. This choice insures that the element displacement functions satisfy the criteria necessary for convergence of the finite element analysis [Ref. 4]. Referring to the curvilinear coordinates (ξ, η, ζ) shown in Figure 1, the rectangular basic x,y,z coordinates at any point in the element are obtained from the NASTRAN basic coordinates at each of the n grid points by:

$$
\left\{ \begin{array}{c} x \\ y \\ z \end{array} \right\} = \sum_{i=1}^{n} N_i \ (\xi, \eta, \zeta) \left\{ \begin{array}{c} x \\ y \\ z \end{array} \right\}_i
\tag{1}
$$

where the $N_i(\xi, \eta, \zeta)$ are shape functions which depend on the number of grid points used to define the element geometry. The N_i functions are either linear quadratic, or cubic, and correspond to employing two, three, or four grid points respectively, along each edge of the element. This choice insures that there are no geometric gaps between grid points. Expressions for the shape functions may be found in Reference 6.

The deformation of the element is represented with the identical interpolating functions used to define the geometry; that is:

$$
\left\{ \begin{array}{c} u \\ v \\ w \end{array} \right\} = \sum_{i=1}^{n} N_i \ (\xi, \eta, \zeta) \left\{ \begin{array}{c} u \\ v \\ w \end{array} \right\}_i
\tag{2}
$$

where u, v and w are displacements along the x, y and z basic coordinate axes. The displacement functions $N_i(\xi, \eta, \zeta)$ satisfy the required convergence criterion of adequately representing a constant strain state, and insure interelement compatibility along the complete element boundary [Ref. 4].

Strain-Displacement Relations

Equation (2) may be used in the well-known strain-displacement relations for a three-dimensional continuum [Ref. 7] to define the strain vector $\{\varepsilon\}$ in terms of the grid point displacements:

$$\{\varepsilon\} = \left[C_1 \mid C_2 \mid \dots \mid C_n \right] \begin{Bmatrix} u_1 \\ v_1 \\ w_1 \\ \hline \vdots \\ \hline u_n \\ v_n \\ w_n \end{Bmatrix} = [C] \{u_e\} \qquad (3)$$

where

$$[C_i] = \begin{bmatrix} \dfrac{\partial N_i}{\partial x} & 0 & 0 \\[2mm] 0 & \dfrac{\partial N_i}{\partial y} & 0 \\[2mm] 0 & 0 & \dfrac{\partial N_i}{\partial z} \\[2mm] \dfrac{\partial N_i}{\partial y} & \dfrac{\partial N_i}{\partial x} & 0 \\[2mm] 0 & \dfrac{\partial N_i}{\partial z} & \dfrac{\partial N_i}{\partial y} \\[2mm] \dfrac{\partial N_i}{\partial z} & 0 & \dfrac{\partial N_i}{\partial x} \end{bmatrix} \qquad (4)$$

In order to evaluate the strain matrix $[C]$, the derivatives of the shape functions N_i with respect to x, y, and z must be calculated. Since N_i is defined in terms of ξ, η and ζ, it is necessary to use the relation that

$$\begin{Bmatrix} \dfrac{\partial N_i}{\partial x} \\[2mm] \dfrac{\partial N_i}{\partial y} \\[2mm] \dfrac{\partial N_i}{\partial z} \end{Bmatrix} = [J]^{-1} \begin{Bmatrix} \dfrac{\partial N_i}{\partial \xi} \\[2mm] \dfrac{\partial N_i}{\partial \eta} \\[2mm] \dfrac{\partial N_i}{\partial \zeta} \end{Bmatrix} \qquad (5)$$

where [J] is the Jacobian matrix. It is easily evaluated by noting that

$$
[J] = \begin{bmatrix} \dfrac{\partial x}{\partial \xi} & \dfrac{\partial y}{\partial \xi} & \dfrac{\partial z}{\partial \xi} \\[2mm] \dfrac{\partial x}{\partial \eta} & \dfrac{\partial y}{\partial \eta} & \dfrac{\partial z}{\partial \eta} \\[2mm] \dfrac{\partial x}{\partial \zeta} & \dfrac{\partial y}{\partial \zeta} & \dfrac{\partial z}{\partial \zeta} \end{bmatrix} = \begin{bmatrix} \dfrac{\partial N_1}{\partial \xi}, & \dfrac{\partial N_2}{\partial \xi}, & \cdots & \dfrac{\partial N_n}{\partial \xi} \\[2mm] \dfrac{\partial N_1}{\partial \eta}, & \dfrac{\partial N_2}{\partial \eta}, & \cdots & \dfrac{\partial N_n}{\partial \eta} \\[2mm] \dfrac{\partial N_1}{\partial \zeta}, & \dfrac{\partial N_2}{\partial \zeta}, & \cdots & \dfrac{\partial N_n}{\partial \zeta} \end{bmatrix} \begin{bmatrix} x_1 & y_1 & z_1 \\ x_2 & y_2 & z_2 \\ \vdots & \vdots & \vdots \\ x_n & y_n & z_n \end{bmatrix} \tag{6}
$$

where the subscripts 1, 2, ... n denote the n grid points of an element.

Stress-Strain Relations

The stress-strain relations for a general elastic material are

$$
\{\sigma\} = [G_e] \{\epsilon - \epsilon_t\} \tag{7}
$$

where $\{\sigma\}$ is the 6x1 stress vector in the basic coordinate system, $[G_e]$ is a 6x6 symmetric elastic material matrix, and $\{\epsilon_t\}$ is the 6x1 thermal strain vector. This thermal strain vector is defined as

$$
\{\epsilon_t\} = \{\alpha_e\} \cdot \sum_{i=1}^{n} N_i \ (\xi,\eta,\zeta) \ T_i \tag{8}
$$

where $\{\alpha_e\}$ is a vector of 6 thermal expansion coefficients, and T_i is the temperature at the ith element grid point.

Stiffness, Mass, and Load Matrices

The stiffness, mass, and load matrices for the isoparametric element are derived by application of the Principle of Virtual Work. These element matrices, relative to the basic coordinate system, are given by

$$
[K_{ee}] = \int_{-1}^{+1} \int_{-1}^{+1} \int_{-1}^{+1} [C]^T \ [G_e] \ [C] \ |J| \ d\xi \ d\eta \ d\zeta \tag{9}
$$

$$
[M_{ee}] = \int_{-1}^{+1} \int_{-1}^{+1} \int_{-1}^{+1} \rho [N]^T \ [N] \ |J| \ d\xi \ d\eta \ d\zeta \tag{10}
$$

$$\{P_e^{\ t}\} \ = \ \int_{-1}^{+1} \int_{-1}^{+1} \int_{-1}^{+1} [C]^T \ [G_e] \ \{\alpha_e\} \ |J| \left(\sum_{i=1}^{n} N_i \ T_i\right) d\xi \ d\eta \ d\zeta \qquad (11)$$

$$\{P_e^{\ P}\} \ = \ - \int_{-1}^{+1} \int_{-1}^{+1} P_{-\zeta} \ [N(\xi,\eta,-1)]^T \ |J| \ \{J_\zeta^{-1}\} \ d\xi \ d\eta$$

$$- \int_{-1}^{+1} \int_{-1}^{+1} P_{-\eta} \ [N(\xi,-1,\zeta)]^T \ |J| \ \{J_\eta^{-1}\} \ d\xi \ d\zeta$$

$$\vdots$$

$$+ \int_{-1}^{+1} \int_{-1}^{+1} P_{+\zeta} \ [N(\xi,\eta,+1)]^T \ |J| \ \{J_\zeta^{-1}\} \ d\xi \ d\eta \qquad (12)$$

where $[K_{ee}]$ is the element stiffness matrix in the basic coordinate system, $[M_{ee}]$ is the mass matrix, $\{P_e^{\ t}\}$ is the thermal load vector, and $\{P_e^{\ P}\}$ is the pressure load vector derived from surface pressures on each of the six faces of the solid element. $|J|$ is the determinant of the Jacobian matrix, and $[N]$ is a matrix of the isoparametric shape function defined by

$$[N] \ = \ \begin{bmatrix} N_1 & 0 & 0 & N_2 & 0 & 0 & & N_n & 0 & 0 \\ 0 & N_1 & 0 & 0 & N_2 & 0 & \cdots & 0 & N_n & 0 \\ 0 & 0 & N_1 & 0 & 0 & N_2 & & 0 & 0 & N_n \end{bmatrix} \qquad (13)$$

$P_{-\zeta}$ is the uniform normal pressure (positive outward) applied to the face of the element where $\zeta = -1$; $P_{-\eta}$ is the pressure applied to the face where $\eta = -1$, etc.; and $\{J_\xi^{-1}\}$, $\{J_\eta^{-1}\}$, and $\{J_\zeta^{-1}\}$ are the first, second, and third columns, respectively, of the inverse of the Jacobian matrix. Products like $|J| \ \{J_\xi^{-1}\}$ in the expression for pressure load are equivalent to a vector of direction cosines multiplied by a surface area scaling factor relating the curvilinear coordinates to the basic coordinate system.

The integrals in equations (9) to (12) are evaluated numerically by using the method of Gaussian Quadrature [Ref. 8]. In the above equations, therefore, [C], $|J|$, and [N] must be evaluated at each interior point used for numerical integration. $[G_e]$, $\{\alpha_e\}$, and ρ can also be evaluated at each integration point. Thus, variations in these quantities are allowed because of, say, temperature-dependent material.

The computations for the isoparametric elements are carried out in the basic coordinate system. If the global coordinate system at any grid point is different from the basic system, the final matrices and vectors are transformed into that global system.

Stress Recovery

The equation for calculating element stresses at any interior point of an isoparametric element may be obtained by combining equations (3), (7), and (8) as follows:

$$\{\sigma\} = [G_e]\left([C]\{u_e\} - \{\alpha_e\} \cdot \left(\sum_{i=1}^{n} N_i T_i\right)\right) \tag{14}$$

$[C]$ and N_i are functions of the element curvilinear coordinates ξ, η, ζ evaluated at the point at which stresses are desired.

Differential Stiffness Matrix

The differential stiffness matrix for the isoparametric solid element is derived by adding the energy of an initial stress state to the potential energy function. This additional energy is derived in Reference 9 and is given by

$$W_p = \frac{1}{2}\int_V \left[\omega_x^2(\sigma_y + \sigma_z) + \omega_y^2(\sigma_x + \sigma_z) + \omega_z^2(\sigma_x + \sigma_y)\right.$$
$$\left. - 2\omega_x\omega_y\tau_{xy} - 2\omega_y\omega_z\tau_{yz} - 2\omega_z\omega_x\tau_{zx}\right]dV \tag{15}$$

where the rotations are given by the relations

$$\left.\begin{array}{l} \omega_x = \frac{1}{2}\left(\dfrac{\partial w}{\partial y} - \dfrac{\partial v}{\partial z}\right) \\[2mm] \omega_y = \frac{1}{2}\left(\dfrac{\partial u}{\partial z} - \dfrac{\partial w}{\partial x}\right) \\[2mm] \omega_z = \frac{1}{2}\left(\dfrac{\partial v}{\partial x} - \dfrac{\partial u}{\partial y}\right) \end{array}\right\} \tag{16}$$

These rotations may be expressed in terms of the grid point displacements by using equation (1):

$$\left\{\begin{array}{c} \omega_x \\ \omega_y \\ \omega_z \end{array}\right\} = \left[\bar{C}_1 \mid \bar{C}_2 \mid \ldots \ldots \mid \bar{C}_n\right]\{u_e\} = [\bar{C}]\{u_e\} \tag{17}$$

428

here

$$[\bar{C}_1] = \frac{1}{2} \begin{bmatrix} 0 & -\dfrac{\partial N_1}{\partial z} & \dfrac{\partial N_1}{\partial y} \\[3mm] \dfrac{\partial N_1}{\partial z} & 0 & -\dfrac{\partial N_1}{\partial x} \\[3mm] -\dfrac{\partial N_1}{\partial y} & \dfrac{\partial N_1}{\partial x} & 0 \end{bmatrix} \tag{18}$$

Substituting equation (17) into equation (15) and adding this function to the potential energy expression yields the differential stiffness matrix:

$$[K_{ee}^d] = \int_{-1}^{+1} \int_{-1}^{+1} \int_{-1}^{+1} [\bar{C}]^T \begin{bmatrix} \sigma_y + \sigma_z & -\tau_{xy} & -\tau_{zx} \\[3mm] -\tau_{xy} & \sigma_x + \sigma_z & -\tau_{zy} \\[3mm] -\tau_{zx} & -\tau_{zy} & \sigma_x + \sigma_y \end{bmatrix} [\bar{C}] \, |J| \, d\xi \, d\eta \, d\zeta \tag{19}$$

As with the structural stiffness matrix, this integral is evaluated using the method of Gaussian Quadrature. The differential stiffness is computed in the basic coordinate system and then transformed, as required, to the NASTRAN global system.

IMPLEMENTATION

Many existing NASTRAN functional modules and subroutines were modified to implement the isoparametric solid elements. Several new subroutines were also added. These modules and brief descriptions of the changes to each are listed in Table 1. The detailed description of these changes presented in Reference 10 can be used to augment the NASTRAN Programmer's Manual instructions, Section 6.8, to assist in the installation of other new elements of similar complexity. Many of the changes are those normally required when implementing new elements. However, in this case, changes were also required in the PLØT module (to plot three-dimensional elements), the GP3 module (to process a new external pressure load), and in various other modules to accommodate the large space requirements of the 32-grid-point cubic element.

It should be noted that the isoparametric elements were installed in functional modules SMA1, SMA2, and DSMG1 on an interim basis only. The element matrix subroutines were designed specifically for the new Element Matrix Generator module and will be made available with Level 16 of NASTRAN.

EVALUATION

A slender cantilever beam model was chosen to evaluate the performance of the three new isoparametric solid elements in NASTRAN. This model was chosen for two reasons: (1) theoretical solutions are well known, and (2) solid finite

429

elements characteristically do not perform well when used to model structures which exhibit predominant bending behavior.

Three models were prepared as shown in Figures 2, 3, and 4, one with each of the three elements: IHEX1, IHEX2, and IHEX3, the linear, quadratic, and cubic elements, respectively. All three beam models had a length (L) of 3.66m (144 in.) and a uniform rectangular cross section with depth (D) of 0.61m (24 in.) and width (W) of 0.30m (12 in.). The same uniform material properties shown in Table 2 were used for all three models. Static, normal modes, and buckling analyses were performed for each of the beam models.

Statics

For the static analyses, all degrees of freedom at the base of the beam (z = 0) were completely fixed. All three models were subjected to the same four loading conditions:

1. Linear thermal gradient (Y-direction)
    T = 322.04 K at Y = 0 (120° F at Y = 0)
    T = 188.71 K at Y = 0.61m (-120° F at Y = 24 in.)

2. Uniform temperature rise
    ΔT = 55.56 K (100° F)

3. Compressive axial pressure (Z-direction)
    P_Z = -2.954 x 10^8 N/m² at Z = 3.66m (-42837 psi at Z = 144 in.)

4. Transverse pressure (Y-direction)
    P_Y = 6.895 x 10^5 N/m² at Y = 0 (100 psi at Y = 0)

The results for the tip displacements are summarized in Table 3, where the computed solutions are compared with the theoretical solutions. The maximum error for the linear IHEX1 element was 10.3% for the transverse pressure load. For the quadratic and cubic elements, IHEX2 and IHEX3, the maximum errors of 4.5% and 3.5%, respectively, occurred in the solutions for the thermal gradient load. For the transverse pressure load, the errors were 1.6% for the IHEX2 element model, and 1.1% for IHEX3. Thus, the higher order isoparametric solid elements perform very well when used to model the bending behavior of this beam.

Normal Modes

In the normal mode analyses, the same single point constraints were applied to all three models in the following manner: All Z components of displacement in the plane Z = 0 and all Y components along the line Z = 0, Y = 0.30m (12 in.), were fixed. For the IHEX1 and IHEX3 models only, all X components along the line Z = 0, X = 0, were fixed. For the IHEX2 model only, the X components along the line Z = 0, X = -0.15m (6 in.), were fixed. This system of constraints was chosen to allow dilatation at the base of the beam. The particular set of constraints used for the IHEX2 model has the additional advantage of symmetry.

430

The inverse power method was used to extract the first three normal modes of each model. The results for the natural frequencies are summarized in Table 4. The computed natural frequencies for the IHEX2 and IHEX3 models are within 3.0 per cent of the theoretical solution. The natural frequency for the IHEX1 model is 2.7% off for bending in the Y-direction, but it is off by 18.3% and 15.8% for the two bending modes about the X-direction. These errors are probably caused by an insufficient number of elements through the width of the beam in the X-direction. Using a smaller mesh size with more IHEX1 elements would improve these results at the expense of increased computer costs. This problem, therefore, serves to demonstrate even more clearly the superiority of the IHEX2 and IHEX3 elements over the IHEX1 element for modeling the bending behavior of structures.

All the computed mode shapes for all three models showed excellent correlation with the theoretical solution [Ref. 11]. Comparative plots of the mode shapes are not included in this paper because there would be no visible distinction between computed and theoretical solutions.

Buckling

Each of the three beam models was used to compute the critical buckling load for axial pressure. The same system of constraints used to compute normal modes was used to compute the axial pressure buckling load. The applied pressure on the end of the beam was -2.954×10^8 N/m^2 (42,837 psi). This amounts to a total applied force of -5.406×10^7 N (-1.234×10^7 lb), which is equal to the theoretical critical load for buckling in the X-direction. Therefore, the fundamental eigenvalue for buckling should have been unity.

Again, the inverse power method was used to extract the three lowest buckling modes. The results for the buckling eigenvalues λ are presented in Table 5. The IHEX2 and IHEX3 element results are excellent. They are within 0.7% of the theoretical solution. The eigenvalue for the IHEX1 element model is in error by less than 10% for buckling in the Y-direction. However, it is off by more than 40% for both buckling modes in the X-direction. This situation is similar to that of the normal mode problem for the IHEX1 element model. Again, it is probably due to the lack of an adequate number of elements through the width of the beam in the X-direction.

As was the case for the normal modes problem, the mode shapes computed by NASTRAN for buckling were very close to the theoretical shapes. Thus, no plots comparing computed shapes with theoretical shapes are included in this paper.

CONCLUDING REMARKS

All three isoparametric solid elements produced good results for static, normal mode, and buckling analyses. As expected, the linear element results showed that it is best used when shear behavior predominates. The superiority of the quadratic and cubic elements was confirmed by the excellent results obtained in both the bending and the shear behavior of a cantilever beam model. Therefore, the implementation of these three isoparametric solid elements, which provide for variations in both material properties and stresses throughout the element, does greatly enhance the total modeling capability of NASTRAN.

431

REFERENCES

1. B. M. Irons, "Engineering Application of Numerical Integration in Stiffness Methods," _AIAA J. 4_, pp. 2035-2037, November 1966.

2. B. M. Irons and O. C. Zienkiewicz, "The Iso-Parametric Element System – A New Concept in Finite Element Analysis," Conf. Recent Advances in Stress Analysis, J.B.C.S.A., Royal Aero. Soc., London, 1968.

3. I. Ergatoudis, "Quadrilateral Elements in Plane Analysis and Introduction to Solid Analysis," M.Sc. Thesis, University of Wales, Swansen, 1966.

4. I. Ergatoudis, B. M. Irons, and O. C. Zienkiewicz, "Curved, Isoparametric, 'Quadrilateral' Elements for Finite Element Analysis," _Int. J. Solids Struct._, Vol. 4, pp. 31-42, 1968.

5. R. W. Clough, "Comparison of Three Dimensional Finite Elements," Symp. Appl. Finite Element Method in Civil Engr., Vanderbilt Univ., Nashville, Tenn., Nov. 1969.

6. O. C. Zienkiewicz, _The Finite Element Method in Engineering Science_, McGraw-Hill, London, p. 121, 1971.

7. S. Timoshenko and J. N. Goodier, _Theory of Elasticity_, 2nd Ed., McGraw-Hill, New York, p. 223, 1951.

8. Z. Kopal, _Numerical Analysis_, 2nd Edition, Chapman and Hill, 1961.

9. R. H. MacNeal, ed., _The NASTRAN Theoretical Manual_, NASA SP-221(01), April 1972.

10. E. I. Field and S. E. Johnson, _Addition of Three-Dimensional Isoparametric Elements to NASA Structural Analysis Program (NASTRAN)_, NASA CR-112269, Jan. 24, 1973.

11. W. C. Hurty and M. F. Rubinstein, _Dynamics of Structures_, Prentice-Hall, Inc., Englewood Cliffs, N.J., 1964.

12. S. P. Timoshenko and J. M. Gere, _Theory of Elastic Stability_, McGraw-Hill, New York, 1961.

TABLE 1.   FUNCTIONAL MODULE MODIFICATIONS TO IMPLEMENT
ISOPARAMETRIC SOLID ELEMENTS

IFP	–	New Bulk Data cards were added
GP2	–	Array sizes were increased to accommodate elements with 32 grid points
PLTSET	–	Array sizes were increased to accommodate elements with 32 grid points
PLØT	–	Capability for plotting solid elements was implemented
GP3	–	Processing of the isoparametric element pressure card was implemented
TA1	–	Capability to append grid point temperatures to EST/ECPT entries was implemented
SMA1	–	Stiffness and conductance matrix generation for the new elements was implemented
SMA2	–	Mass and capacitance matrix generation for the new elements was implemented
SSG1	–	Load vector generation for thermal and pressure loads on the new elements was implemented
DSMG1	–	Differential stiffness matrix generation for the new elements was implemented
SDR2	–	Stress calculations for individual grid points of the new elements was implemented
ØFP	–	Stress printout formats for the new elements were implemented

TABLE 2. MATERIAL PROPERTIES OF THE CANTILEVER BEAM MODELS

Symbol	Description	Value (SI)	Value (English)
E	Young's modulus	2.068×10^{11} N/m^2	30×10^6 lb/in^2
ν	Poisson's ratio	0.3	0.3
α	Coef. of thermal expansion	$2.570 \times 10^{-5} \frac{m}{m - {}^\circ K}$	$1.428 \times 10^{-5} \frac{in}{in - {}^\circ F}$
ρ	Mass density	20.86 kg/m^3	7.535×10^{-4} lb/in^3

TABLE 3. COMPARISON OF TIP DEFLECTIONS FOR NASTRAN AND THEORETICAL
SOLUTIONS FOR FOUR STATIC LOADING CONDITIONS

Load Case	Description	NASTRAN Solutions						Theoretical Solution*
		IHEX1 Model		IHEX2 Model		IHEX3 Model		Solution*
		Defl., cm	Error, %	Defl., cm	Error, %	Defl., cm	Error, %	Tip Defl., cm
1	Thermal Gradient	3.668	2.5	3.932	4.5	3.894	3.5	3.762
2	Uniform Temperature	.5367	2.8	.5344	2.3	.5304	1.6	.5222
3	Axial Compression	-.5179	0.8	-.5187	0.7	-.5199	0.4	-.5222
4	Transverse Pressure	.3612	10.3	.3965	1.6	.3985	1.1	.4028

*Theoretical Solutions

Load Case 1

$$\delta_Y = \frac{\alpha \Delta T L^2}{2D}$$

$\delta_Y = 3.762$ cm

Load Case 2

$$\delta_z = \alpha \Delta T L$$

$\delta_Y = .5222$ cm

Load Case 3

$$\delta_z = \frac{P_z L}{E}$$

$\delta_Y = -.5222$ cm

Load Case 4

$$\delta_Y = \frac{3P_Y L^4}{2ED^3} \left[1 + \frac{4D^2}{5L^2} \right]$$

$\delta_Y = .4028$ cm

TABLE 4.   COMPARISON OF NATURAL FREQUENCIES FOR NASTRAN AND
THEORETICAL SOLUTIONS

Mode	Description	NASTRAN Solutions						Theoretical Solution, cps [Ref. 11]
		IHEX1 Model		IHEX2 Model		IHEX3 Model		
		Freq., cps	Error, %	Freq., cps	Error, %	Freq., cps	Error, %	
1	First Bending Mode in the X-Direction	22.0	18.3	18.6	0	18.6	0	18.6
2	First Bending Mode in the Y-Direction	38.3	2.7	36.5	2.1	36.5	2.1	37.3
3	Second Bending Mode in the X-Direction	135.3	15.8	114.3	2.1	113.3	3.0	116.8

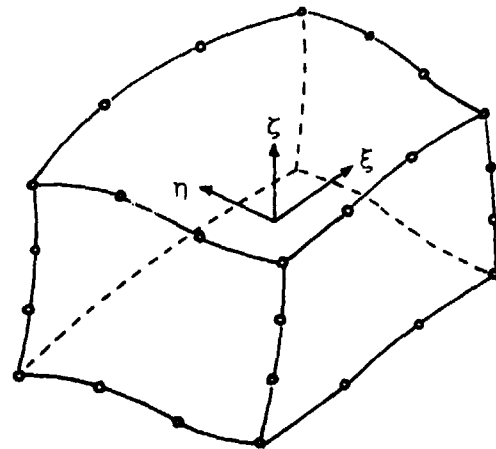TABLE 5.   COMPARISON OF BUCKLING EIGENVALUES FOR NASTRAN AND
THEORETICAL SOLUTIONS

Mode	Description	NASTRAN Solutions						Theoretical Solution λ [Ref. 12]
		IHEX1 Model		IHEX2 Model		IHEX3 Model		
		λ	Error, %	λ	Error, %	λ	Error, %	
1	X-Direction	1.406	40.6	1.002	.2	1.001	.1	1.0
2	Y-Direction	4.391	9.8	3.981	.5	3.979	.5	4.0
3	X-Direction	12.809	42.3	9.037	.4	8.934	.7	9.0
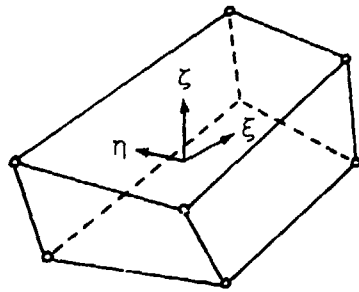
(a) Linear.
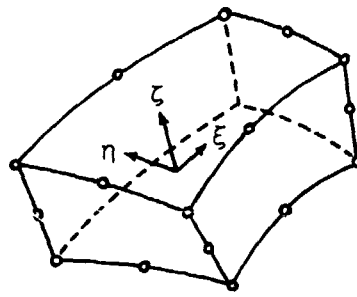
(b) Quadratic.

(c) Cubic

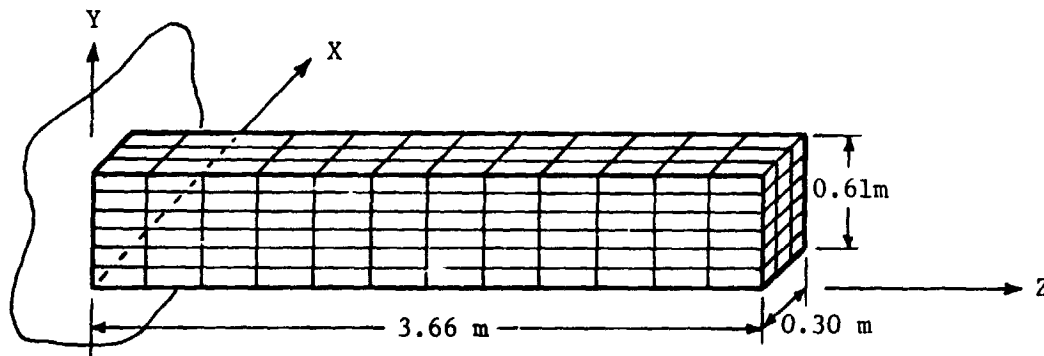FIGURE 1.   THREE ISOPARAMETRIC ELEMENTS

436

FIGURE 2.   IHEX1 MODEL -- 216 ELEMENTS AND 364 GRID POINTS
MATRIX ORDER (g-SET) = 1092, SEMI-BANDWIDTH = 102.
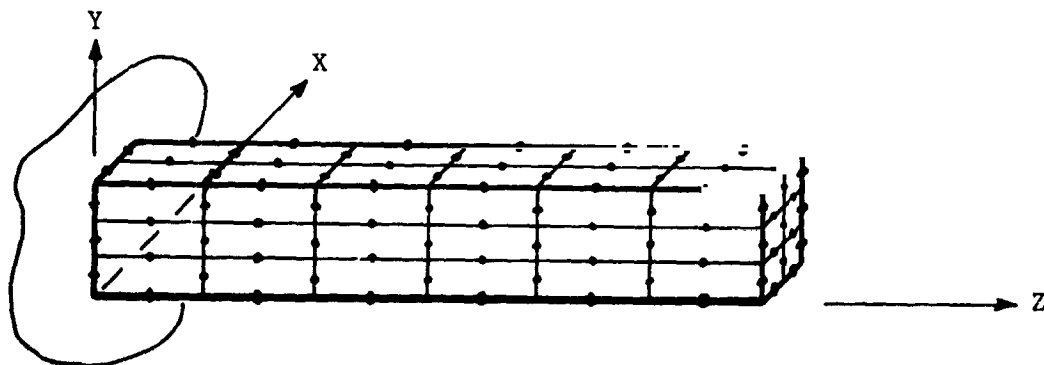

FIGURE 3.   IHEX2 MODEL -- 36 ELEMENTS AND 275 GRID POINTS
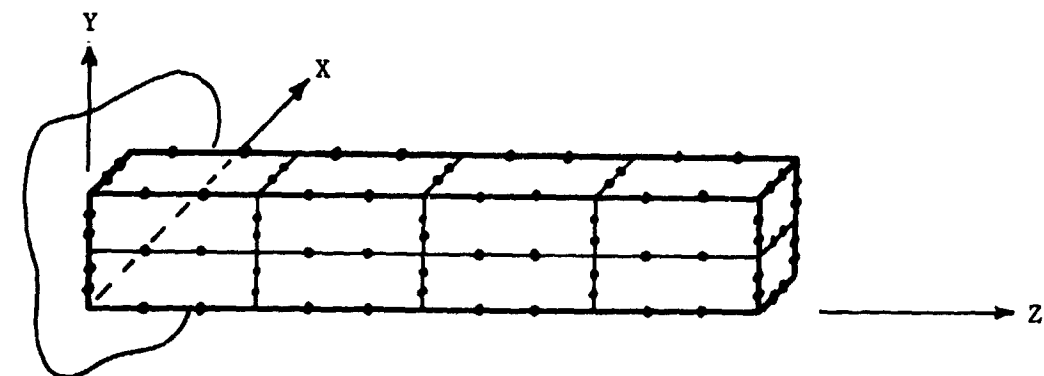MATRIX ORDER (g-SET) = 825, SEMI-BANDWIDTH = 156.

FIGURE 4.   IHEX3 MODEL -- 8 ELEMENTS AND 148 GRID POINTS
MATRIX ORDER (g-SET) = 444, SEMI-BANDWIDTH = 132.